# Page Proof Instructions and Queries

Thank you for choosing to publish with us. This is your final opportunity to ensure your article will be accurate at publication. Please review your proof carefully and respond to the queries using the circled tools in the image below, which are available **by clicking "Comment"** from the right-side menu in Adobe Reader DC.*

Please use *only* the tools circled in the image, as edits via other tools/methods can be lost during file conversion. For comments, questions, or formatting requests, please use ⊺ Please do *not* use comment bubbles/sticky notes 💬.
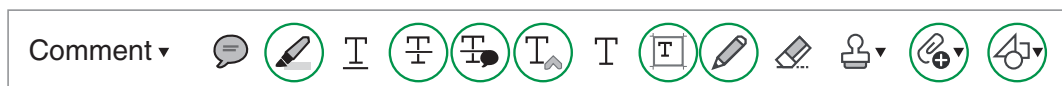


*If you do not see these tools, please ensure you have opened this file with Adobe Reader DC, available for free at get.adobe.com/reader or by going to Help > Check for Updates within other versions of Reader. For more detailed instructions, please see us.sagepub.com/ReaderXProofs.

| No. | Query |
|---|---|
|  | Please confirm that all author information, including names, affiliations, sequence, and contact details, is correct. |
|  | Please review the entire document for typographical errors, mathematical errors, and any other necessary corrections; check headings, tables, and figures. |
|  | Please confirm that the Funding and Conflict of Interest statements are accurate. |
|  | Please ensure that you have obtained and enclosed all necessary permissions for the reproduction of artistic works, (e.g. illustrations, photographs, charts, maps, other visual material, etc.) not owned by yourself. Please refer to your publishing agreement for further information. |
|  | Please note that this proof represents your final opportunity to review your article prior to publication, so please do send all of your changes now. |
| AQ: 1 | Per journal style, abstracts should not have reference citations. Therefore, year '2015' after the reference citation 'Semiletov et al.' has been deleted. |
| AQ: 2 | Please provide at least 3–5 keywords for this manuscript. |
| AQ: 3 | Please note that name-date citations have been changed to numbered citations per journal style. |
| AQ: 4 | Please provide the publisher location for references 1, 7, 15, 18, and 23. |
| AQ: 5 | Please provide complete page range for references 3 and 9. |
| AQ: 6 | Please provide the publisher name and location for references 19, 27, and 30. |
| AQ: 7 | Please provide History dates for the article |

# Similarity scaling of jet noise sources for low-order jet noise modelling based on the Goldstein generalised acoustic analogy

## Vasily A Semiletov[1] and Sergey A Karabasov[2]

### Abstract

As a first step towards a robust low-order modelling framework that is free from either calibration parameters based on the far-field noise data or any assumptions about the noise source structure, a new low-order noise prediction scheme is implemented. The scheme is based on the Goldstein generalised acoustic analogy and uses the Large Eddy Simulation database of fluctuating Reynolds stress fields from the CABARET MILES solution of Semiletov et al. corresponding to a static isothermal jet from the SILOET experiment for reconstruction of effective noise sources. The sources are scaled in accordance with the physics-based arguments and the corresponding sound meanflow propagation problem is solved using a frequency domain Green's function method for each jet case. Results of the far-field noise predictions of the new method are validated for the two NASA SHJAR jet cases, sp07 and sp03 from and compared with the reference predictions, which are obtained by applying the Lighthill acoustic analogy scaling for the SILOET far-field measurements and using an empirical jet-noise prediction code, sJet. [AQ1]

## Introduction

Many flow characteristics of single-stream turbulent jets, such as the axial velocity profile, the shear layer width and the lipline distribution of turbulent velocity fluctuations collapse to

[1]Department of Engineering, University of Cambridge, Cambridge, UK
[2]School of Engineering and Materials Science, Queen Mary University of London, London, UK

**Corresponding author:**
Vasily A Semiletov, Department of Engineering Cambridge, University of Cambridge, Cambridge CB3 0DYCB3, UK.
Email: ananya.pathak@sagepub.in

certain dimensionless profiles when scaled by jet parameters such as nozzle exit velocity, coflow velocity, nozzle diameter and potential core length.[1–3] **[AQ3]**

Examples of such data collapse are shown in Figure 1(a) and (b), which present the dimensionless centreline axial meanflow velocity and turbulent velocity intensity profiles, respectively. All data are plotted along the axial distance from the nozzle exit and normalised by the jet potential core length $X_c$. The jet conditions correspond to the SILOET experiment performed in the Noise Test Facility (NTF) of QinetiQ. These are three jets: one static isothermal, one static heated jet at temperature ratio $T_j/T_0 = 2.5$ and the same isothermal jet at coflow of $U_{coflow}/c_0 = 0.3$. All jets correspond to acoustic Mach number $M_a = U_j/c_0 = 0.875$ and the same single-stream convergent nozzle of diameter, $D_j$ equal to 0.1016 m. Here $T_j$, $T_0$, and $c_0$ are jet static temperature, ambient static temperature and ambient sound speed, respectively. For the isothermal jet, these conditions correspond to Reynolds number based on the nozzle diameter of about $2 \times 10^6$.

The flow solutions have been obtained with the MILES CABARET code[4–6] on a hexahedral cylindrical grid of circa $21 \times 10^6$ cells in total. Computation details are available in Semiletov et al.[7] All three jet flow solutions tend to collapse to the same similitude profiles both for the means and the fluctuations except for the initial spike of the root-mean-square (r.m.s.) velocity fluctuation profile caused by the initially laminar LES solution due to a lack of the grid resolution. Note that the dimensionless meanflow velocity profiles are also in a good agreement with the empirical function of Witze.[4]

In comparison with jet aerodynamics, quantities relevant for jet acoustics correspond to higher-order statistical moments. Starting from the pioneering work of Lighthill,[8] many acoustic analogy formulations for jet mixing noise modelling are based on re-arranging the original Navier–Stokes equations into a linear sound propagation operator and non-linear source terms. Classical examples include the formulations by researchers.[9–12] The most complete formulation in the sense of accurate delineation of sound meanflow propagation and generation effects corresponds to the generalised acoustic analogy model by Goldstein.[13] This model, which was further developed in Goldstein and Leib,[14] exactly rearranges the governing Navier–Stokes equations to arrive at a set of nominally linear hyperbolic propagation equations with the non-linear sound sources on the right-hand-side. This re-arrangement reduces the non-linear sources to covariance of non-linear fluctuating stresses terms,
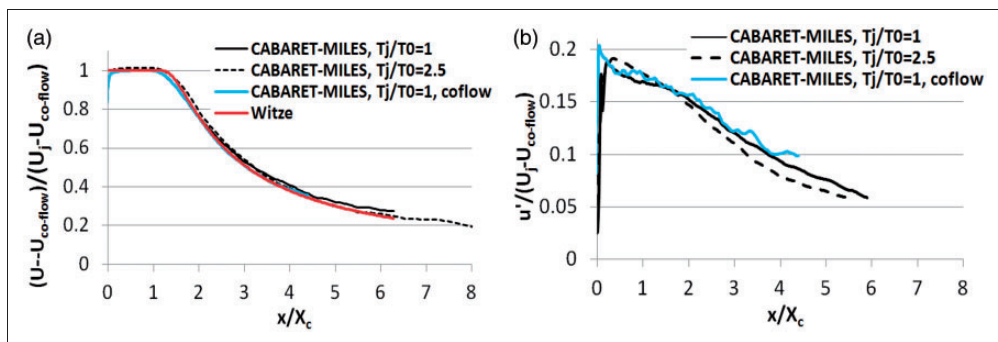


**Figure 1.** Similarity scaling of jet centerline velocity (a) and r.m.s. velocity fluctuations along the lipline (b) based on jet velocity at the nozzle exit, coflow velocity and potential core length of the jet.

which are much simpler for calculation in comparison with the sources of the classical acoustic analogies such as those by Lighthill or Lilley.

The auto-covariance functions of the generalised fluctuating Reynolds stress tensor, which corresponds to the effective noise sources of the Goldstein acoustic analogy, are shown both experimentally[15,16] and computationally[1,17,18] to collapse to similitude curves for a wide range of jet Mach numbers when non-dimensionalised appropriately.

The similarity of the fourth-order correlations can be the basis for developing the low-order models for jet noise in the literature not necessarily only limited to the Goldstein generalised acoustic analogy. This can be achieved by scaling the corresponding parameters of the correlation model, e.g. as the space, time scales and amplitudes of various components of the covariance of fluctuating Reynolds stresses, based on the meanflow and turbulence quantities obtainable from the RANS solutions of the same jets.[17,19,20,21] Unfortunately, unlike for the aerodynamic data, the number of 'measurement points' where such as covariance functions of fluctuating turbulent stresses relevant for jet acoustics are available for acoustic modelling is typically very limited. This is true both for the experiment and eddy-resolving (e.g. Large Eddy Simulation (LES)) computational modelling[22–25] and leads to unwanted assumptions and artificial calibration parameters based on the far-field noise measurements, which implicitly involves some (unwanted) scaling of the far-field propagation effects and makes the entire low-order jet noise prediction scheme less robust.

The goal of the current paper is to make the first step in the direction of low-order modelling framework based on the acoustic analogy that is free either from the calibration parameters based on far-field noise data or any assumptions about the noise source structure. The starting point of this work is the database of LES solutions corresponding to the static isothermal SILOET jet from Semiletov et al.[1] The latter work offered a new implementation of the Goldstein generalized acoustic analogy model based on extracting the second-order fluctuating turbulent stresses from LES for direct computation of the far-field acoustic pressure. The new method was validated in comparison with the far-field noise spectra measurements available. The implementation didn't require any assumptions about the functional dependence of the covariance of fluctuating stress terms in comparison with the previous studies.

In the present paper, the same database of fluctuating Reynolds stress fields as extracted from the static isothermal SILOET jet solution of Semiletov et al.[1] is used for low-order modelling of other jet cases for which no LES solution is readily available. For reference, the original implementation of Semiletov et al.[1] was based on computing the far-field pressure in the observer reference frame, which main steps are summarised below:

(a) Perform the LES simulation,
(b) Either during or as a post-processing step calculate the mean flow properties as well as the fluctuating stress tensor components,
(c) Calculate the adjoint Green's function for every cell in the computational domain based on a locally parallel flow approximation,
(d) Evaluate all nine components of the fluctuating Reynolds stress tensor in the entire jet volume,
(e) Break the time domain signal of each fluctuating stress field into several overlapping intervals in accordance with the signal processing and transform each signal into the frequency domain,

(f) Integrate the volume integral to obtain the complex pressure signal for each statistical interval,

(g) Calculate the power spectral density from the complex pressure signals by averaging over all realisations.

In the present work, there is no step (a) or (b). Instead, using the source scaling arguments, the LES flow solutions for turbulent stresses available from Semiletov et al.[1] will be modified for reconstructing the effective noise sources of two static isothermal NASA SHJAR jets from Bridges and Wernet[26] along the steps (c)–(g). The jet cases under consideration here are the so-called Setpoint 7 and 3, sp07 and sp03, which are static isothermal jets corresponding to the acoustic Mach number $M_a = U_j/c_0 = 0.9$ and 0.5, respectively. The nozzle is convergent and contoured with diameter $D_j = 0.0508$ m (SMC000). Wind-US RANS solutions[27] will be used for obtaining the meanflow fields of the jets and, consequently, for solving the meanflow propagation problem in the frequency domain for a few representative far-field observer locations in each case. The resulting Green's function will be integrated with the reconstructed sources to obtain the acoustic pressure spectra at the far field. For validation, all noise spectra predictions will be compared with the far-field noise data from the NASA SHJAR experimental database.

## Governing acoustic analogy equations

The Goldstein generalised acoustic analogy equations[13,14] are summarised below.

By introducing the fluctuation density, pressure, enthalpy and velocity variables, so that

$$\rho' \equiv \rho - \bar{\rho}, \ \ p' \equiv p - \bar{p}, \ \ h' \equiv h - \bar{h}, \ \ v_i' \equiv v_i - \bar{v}_i \tag{1}$$

where bar and tilde represent time and Favre averaging and using generalised pressure and momentum variables

$$
\begin{aligned}
p_e' &\equiv p' + \frac{\gamma - 1}{2}\left(\rho v'^2 - \bar{\rho}\widetilde{v'^2}\right), \\
u_i &\equiv \rho v_i'
\end{aligned}
\tag{2}
$$

the Navier–Stokes equations are exactly rearranged to the following nominally linear form

$$
\begin{aligned}
&D_0\rho' + \nabla_j u_j = 0, \\
&D_0 u_i + u_i\nabla_j\tilde{v}_i + \nabla_i p_e' - \frac{\rho'}{\bar{\rho}}\nabla_j\tilde{\theta}_{ij} = \nabla_i e_{ij}'', \\
&D_0 p_e' + \nabla_j\widetilde{c^2}u_j + (\gamma - 1)\left(p_e'\nabla_j\tilde{v}_j - \frac{u_i}{\bar{\rho}}\nabla_j\tilde{\theta}_{ij}\right) = \nabla_j e_{4j}'' + (\gamma - 1)e_{ij}''\nabla_j\tilde{v}_i,
\end{aligned}
\tag{3}
$$

where

$$
\begin{aligned}
D_0 &\equiv \frac{\partial}{\partial t}\cdot + \nabla_j(\tilde{v}_j\cdot) \\
\tilde{\theta}_{ij} &\equiv \delta_{ij}\bar{p}_e - \overline{e_{ij}'}, \\
v_4' &\equiv (\gamma - 1)\left(h' + \tfrac{1}{2}v'^2\right) = \left(c^2\right)' + \tfrac{\gamma-1}{2}v'^2, \\
e_{vj}'' &\equiv -\rho v_v' v_i' + \delta_{ij}\tfrac{\gamma-1}{2}v'^2 + \left(\sigma_{ij} + (\gamma - 1)\delta_{v4}\sigma_{ik}v_k'\right),
\end{aligned}
\tag{4}
$$

and where $\tilde{c}^2$ is the square of the mean-flow sound speed and $\tilde{\theta}_{ij}$ is the total mean flow stress tensor. The source tensor components, $e''_{vj}$, $v = 1, 2, 3, 4$ and $j = 1, 2, 3$ (indices 1,2,3 correspond to the fluctuating Reynolds stresses and index 4 corresponds to the fluctuating enthalpy source) are given by

$$e''_{\mu j} \equiv e'_{\mu j} - \overline{e'_{\mu j}}.$$

The above fluctuating turbulent stresses are the output, which can be obtained from LES such as in Semiletov et al.[1]

As commonly accepted in acoustic analogy modelling, the nonlinear sources are assumed to exclude the acoustic variable and the far-field acoustic pressure solution is obtained as a convolution integral of the Green's function with the nominal sources

$$p(\boldsymbol{x}, t) = \int_{-T}^{T} \int_{V} \left( e''_{ij}(\boldsymbol{y}, \tau) \nabla_i u'_j(\boldsymbol{y}, \tau | \boldsymbol{x}, t) \right) \mathrm{d}\boldsymbol{y} \mathrm{d}\tau$$
$$- \int_{-T}^{T} \int_{V} \left( e''_{4j}(\boldsymbol{y}, \tau) \nabla_j p'(\boldsymbol{y}, \tau | \boldsymbol{x}, t) - (\gamma - 1) e''_{ij}(\boldsymbol{y}, \tau) p'(\boldsymbol{y}, \tau | \boldsymbol{x}, t) \nabla_j \tilde{v}_i(\boldsymbol{y}) \right) \mathrm{d}\boldsymbol{y} \mathrm{d}\tau$$

(5)

where $p$ is far-field pressure and $u'_j$ and $p'$ are components of the vector adjoint Green's function for momentum and pressure, $T$ denotes the time interval and $V$ is the jet volume. Applying integration by parts and introducing a single notation for the Green's function propagator tensor,[14] the acoustic integral is rearranged to

$$p(\boldsymbol{x}, t) = \int_{-T}^{T} \int_{V} e''_{\mu j}(\boldsymbol{y}, \tau) \Gamma_{\mu j}(\boldsymbol{y}, \tau | \boldsymbol{x}, t) \mathrm{d}\boldsymbol{y} \mathrm{d}\tau$$

(6)

Then the far-field pressure power $P(\boldsymbol{x}, t) = p(\boldsymbol{x}, t) p(\boldsymbol{x}, t)^*$, where * represents complex conjugate can be written in terms of the integral of covariance of the fluctuating stresses

$$\mathrm{R}_{ijkl}(\boldsymbol{y}, \Delta \boldsymbol{y}, \tau) = \frac{1}{2T} \int_{-T}^{T} e''_{ij}(\boldsymbol{y}, t) e''_{kl}(\boldsymbol{y} + \Delta \boldsymbol{y}, t + \tau) \mathrm{d}t$$

(7)

For isothermal jets, such as the ones considered for this publication, the source terms corresponding to the enthalpy fluctuations can be neglected and covariance functions of the fluctuating Reynolds stress components $(i, j, k, l = 1, 2, 3)$ become the only relevant source terms.

The propagator tensor $\Gamma_{\mu j}(\boldsymbol{y}, \tau | \boldsymbol{x}, t)$ depends on the adjoint vector Green's function components and generally requires solving linearised Euler equations. In the current work, a simplified locally parallel flow approximation is used to solve the sound meanflow propagation problem similar to Goldstein and Leib.[14] The former approximation for solving the sound meanflow propagation problem was also shown to work reasonably well for the same jets by Semiletov et al.[1]

Briefly, under the locally parallel flow approximation, the jet flow is divided into a series of non-overlapping sections along the jet stream-wise coordinate. Each of the sections is stream-wise averaged to correspond to a piece-wise constant flow field in terms of the stream-wise coordinate that becomes a function of radius only, e.g. $\tilde{v} = (\tilde{v}(r), 0, 0)$. For each jet section, periodic boundary conditions are assumed in the stream-wise direction. After such simplifications, the linearised Euler equations can be solved for each azimuthal mode separately, which leads to an ordinary differential equation of Rayleigh type for the

amplitude of each mode as a function of radius. Overall, these amplitudes will be a function of both radius and axial location because of the local meanflow velocity profile used. Details of the parallel flow sound propagation solution for isothermal jets can be found in Tam and Auriault.[28]

Having computed the amplitude of each component of the vector adjoint Green's function at each axial and radial location, we reconstruct the three-dimensional adjoint Green's function as a function of radius, axial location and azimuthal angle: each amplitude is multiplied by the corresponding Fourier function of the azimuthal mode and the result is added together with the rest of other modal contributions. The adjoint Green's function is typically computed in the frequency domain for a discrete set of frequencies. Hence, for example, to obtain a time-domain adjoint Green's function propagator required in far-field pressure integral (5), the corresponding three-dimensional time-domain Green's function can be reconstructed by inverse Fourier transform. This is how the far-field pressure solutions have been obtained in the current paper following Semiletov et al.[1]

The above is a general way to proceed in case the source from the LES data have to be stored in a 3D volume as it would be the case for asymmetric jets. As a side note, an alternative post-processing method, which is most storage effective in case of axi-symmetric jet flows, is to decompose the sources in (5) obtained from LES into separate azimuthal modes and record them mode-by-mode rather than in a 3D volume. Then it is only the amplitude component of the vector adjoint Green's function solution, which is needed for each axial and radial location because of azimuthal mode decoupling in the sound power integral and direct correspondence between the adjoint Green's function mode and the source mode for axi-symmetric jets.

Another interesting side note to make here is that Semiletov et al.[1] showed that within their noise source modelling approach directly based on LES, which avoids usual intermediate assumptions about various noise source components, the above locally parallel jet model does not appear to be such a bad approximation of the full spreading jet propagation equations for unheated subsonic jets at least. This is contrary to conclusions of some of the previous works on the Goldstein acoustic analogy based on modelling of the fourth-order correlations.[17,22]

## Acoustic source scaling

For $90°$ angle to the jet flow, meanflow propagation effects are negligible and the locally parallel Green's flow solution coincides with the analytical free-space solution that can be used for computing the far-field acoustic power spectra by convoluting the Green's function operator the auto-covariance of Reynolds stress tensor, $R_{ijkl}$.

In Semiletov et al.,[1] it was shown that for static isothermal SILOET jet, it is only the $R_{2222}$ component (1 in the jet axis direction, 2 is the radial jet direction of the cylindrical-polar coordinate system) that is important for far-field noise at $90°$ polar angle. Furthermore, in Semiletov and Karabasov,[29] the following features of covariance of Reynolds stresses corresponding to an isothermal jet flow were demonstrated:

- All three major correlation components, $R_{1111}$, $R_{2222}$ and $R_{1212}$, collapse to several 'universal' profiles when normalised by the temporal and spatial correlation scales and the nozzle exit velocity in accordance with the NASA SHJAR experiment,

- The following model

$$R_{ijkl}(\mathbf{y}, \Delta \mathbf{y}, \tau) \sim \exp\left(-\sqrt[2]{\left(\frac{|U_c\tau|}{L_\tau}\right)^2 + \left(\frac{|\Delta y_1 - U_c\tau|}{L_1}\right)^{2.5} + \left(\frac{|\Delta y_2|}{L_2}\right)^{2.5} + \left(\frac{|\Delta y_3|}{L_3}\right)^{2.5}}\right) \quad (8)$$

where $(L_\tau, L_1, L_2, L_3)$ are the corresponding correlation scales in the temporal, $\tau$ and spatial directions, $y_1, y_2, y_3$ in the nozzle-fixed coordinate system, and where $U_c$ is the eddy convection velocity, provides a good approximation for the SILOET jet noise source data as reconstructed from the LES solution of Semiletov et al.;[1] the correlation lengthscales can be further scaled based on the jet diameter and the sound frequency (also in agreement with Leib and Goldstein[21]),

- The eddy convection velocity, $U_c$, as obtained from the LES solution in the jet shear layer region is close to the local meanflow velocity.

$$\overline{p(\mathbf{x}, \omega)\, p^*(\mathbf{x}, \omega)} = \frac{\omega^4}{(4\pi \tilde{c}^2 R)^2} \int_{V_y} \int_{V_{\Delta y}} \int_{-\infty}^{+\infty} R_{2222}\left(\frac{U_j\tau}{D_j}, \frac{x}{D_j}, \frac{y}{D_j}, \frac{z}{D_j}\right) e^{i\omega\tau - \frac{i\omega}{c}r}\, \mathrm{d}\tau \mathrm{d}\Delta y \mathrm{d}y, \quad (9)$$

where R is the distance from the jet to the far-field observer at $\mathbf{x}$ and $\omega$ is sound frequency.

Following Lighthill, a simple dimensional analysis can be performed based on the following scaling: $\omega \sim U_j/D_j$, $L_i \sim D_j$, $V_y \sim D_j^3$ and $|R_{2222}| \sim U_j^4$. Also, from $R_{2222} = f\left(\frac{U_j\tau}{D_j}, \frac{x}{D_j}, \frac{y}{D_j}, \frac{z}{D_j}\right)$ and using a property of the Fourier Transform such that if $\hat{f}(\omega) = \int_{-\infty}^{+\infty} f(t)e^{i\omega t}\, \mathrm{d}t$, then $\int_{-\infty}^{+\infty} f(\alpha t)e^{i\omega t}\, \mathrm{d}t = \frac{1}{\alpha}\, \hat{f}\left(\frac{\omega}{\alpha}\right)$, the inner time integral in (9) leads to an additional multiplier $D_j/U_j$. Combining these together leads to the following scaling law for the physical acoustic spectra

$$\overline{p(\mathbf{x}, \omega)\, p^*(\mathbf{x}, \omega)} \sim \omega^4 |R_{2222}| L_1 L_2 L_3 \frac{1}{\omega} V_y/R^2 \sim \left(\frac{U_j}{D_j}\right)^4 \frac{D_j}{U_j} U_j^4 D_j^3 D_j^3/R^2 = \frac{U_j^7 D_j^3}{R^2} \quad (10)$$

or

$$\overline{p(\mathbf{x}, \omega)\, p^*(\mathbf{x}, \omega)} \sim \frac{U_j^8 D_j^2}{R^2}/f_{ref} \quad (11)$$

in terms of the acoustic power spectra normalised by reference frequency $f_{ref} = \frac{U_j}{D_j}$.

Equation (11) gives identically the same scaling law as the one that was obtained by Lighthil.[8] This coincidence is not surprising since for subsonic isothermal jets (where the sound speed is approximately constant) and with neglecting meanflow propagation effects the Goldstein acoustic analogy reduces to Lighthill's acoustic analogy model.

Figures 2 and 3 show how the Lighthill scaling based on $\frac{U_j^8 D_j^2}{R^2}$ performs if one uses it to compare the sound spectra measurements corresponding to the static isothermal SILOET jet ($R = 120D_j$) with the NASA SHJAR spectra for sp07 and sp03 jets ($R = 100D_j$) using the dimensionless frequency with the Strouhal number based on the jet diameter $St = fD_j/U_j$. The predictions of sJet code[30] are shown on the same plots for comparison. The latter are
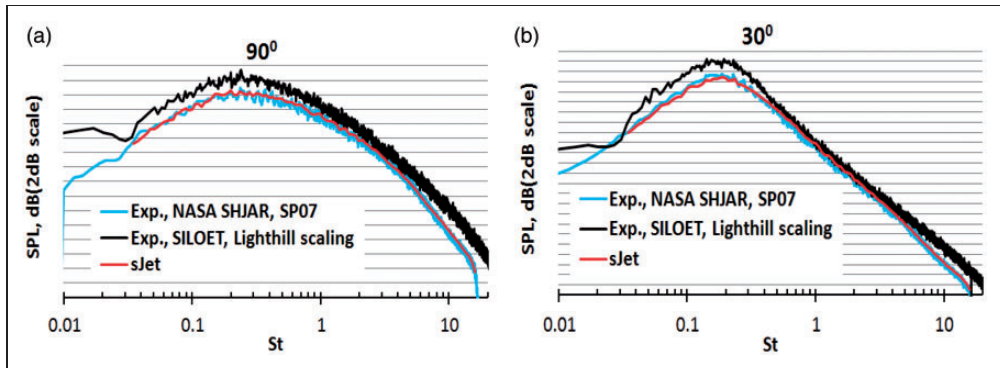
**Figure 2.** Comparison of noise spectra from the SILOET experiment scaled in accordance with the Lighthill theory and sJet predictions with the NASA SHJAR sp07 noise measurements for (a) 90° and (b) 30° observer angle to the jet flow.
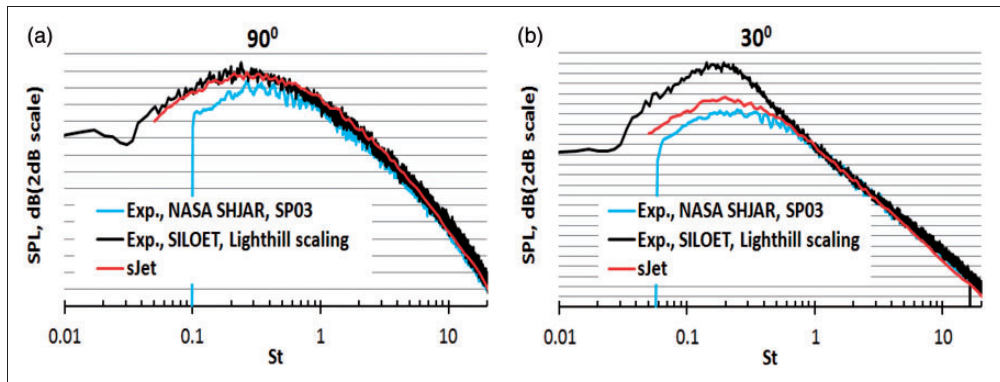SPL: sound pressure level.



**Figure 3.** Comparison of the noise spectra from the SILOET experiment scaled in accordance with the Lighthill theory and sJet predictions with the NASA SHJAR sp03 noise measurements for (a) 90° and (b) 30° observer angle to the jet flow.
SPL: sound pressure level.

not based on any physical model but use empirical scaling functions calibrated using the experimental jet noise database for a range of acoustic Mach numbers, $M_a$ from 0.67 to 1.09.

It can be observed that the Lighthill scaling reproduces the correct sp07 spectra within 2 dB for both 90° and 30° angles to the jet flow.

Note that the latter case that corresponds to $M_a = 0.9$ is not a real challenge for the acoustic analogy model since the SILOET LES data used as reference for the scaling correspond to similar Mach number, $M_a = 0.875$. It is only the difference in jet diameter between the SILOET and the NASA jet case, which can contribute to the scaling appreciably in this case. In contrast to this, the sp03 case, which corresponds to $M_a = 0.5$, represents quite a stretch for the Lighthill acoustic analogy model. For this jet, it is only the 90° spectra,

which are captured by Lighthill's scaling within 2 dB from the reference experiment. The predictions for 30° polar angle, obtained with the same scaling, are amplified by as much as 8–10 dB at peak noise frequencies. The latter is not surprising: the celebrated Lighthill's $v^8$ law has well-known limitations and, in particular, cannot be correct at small polar angles.[31]

In comparison with the Lighthill scaling, the sJet predictions based on empirical scaling laws are much more accurate: they are 'spot on' for NASA SHJAR sp07 jet case (in fact, the sJet solution in this case looks like a smoothed version of the experimental data from which it was derived), and remain within 2–3 dB from the experiment for the lower speed sp03 jet case. Still, the 2–3 dB accuracy in case of the sp03 jet case including the spectra predictions for 30° angle is a significant improvement compared to the classical Lighthill acoustic analogy result. In the next section, we will see how the acoustic analogy results can be improved by taking into account meanflow sound propagation effects in accordance with the Goldstein model.

## Results of low-order acoustic modelling

In comparison with Lighthill's acoustic analogy, a key feature of the Goldstein acoustic analogy is its accounting for sound meanflow propagation effects. Therefore, in the current low-order implementation of this model, it is only the fluctuating stress tensor components, which are scaled in accordance with the jet flow case under consideration, e.g. $e''_{vj} \sim U_j^2$, $V_y \sim D_j^3$, $\omega \sim U_j/D_j$ using the LES solutions for the SILOET jet but no scaling law is applied for solving the sound meanflow propagation problem. The meanflow propagation problem is solved for each jet conditions based on the RANS meanflow solutions available (Towne, 2009) by using the locally parallel flow Green's function method. That is, importantly, there is not any scaling assumption applied for the meanflow sound propagation modelling. Because of the fast solution times, the propagation problem is solved explicitly for each jet flow in question.

First, acoustic modelling results for the sp07 jet case are discussed. Figure 4(a) and (b) shows the far-field spectra predictions of the new low-order model that is based on scaling the effective sound sources of the Goldstein acoustic analogy and using the locally parallel Green's function with the RANS-based meanflow for 90° and 30° angle to the jet flow, respectively. Results of applying the Lighthill scaling to the spectra measurements from the SILOET experiment (for 90° only) are shown on the same plot for comparison. Note that both the new low-order model and the standard Lighthill scaling lead to a similar accuracy within 2–3 dB from the experiment for 90° observer angle to the jet for a good range of frequencies upto St = 2–3. For 30° angle, noise spectra predictions of the current low-order model are within 1 dB from the experiment for the same frequency range.

To understand the 2–3 dB discrepancy of the current low-order model with the experiment at 90° observer angle, it is worth recalling the previous MILES CABARET predictions based on the same LES and the Goldstein generalised acoustic analogy implementation from Semiletov et al.[1] The latter solutions are shown in Figure 5 compared to the far-field noise predictions based on the standard permeable surface Ffowcs Williams–Hawkings method (1969) with the same LES data.

For most frequencies upto St = 2, which approximately demarcates the resolution limit of the LES grid from Semiletov et al.[1] as shown in Figure 6, the agreement between the spectra predictions of the two methods based on the same LES solution is within 1 dB.
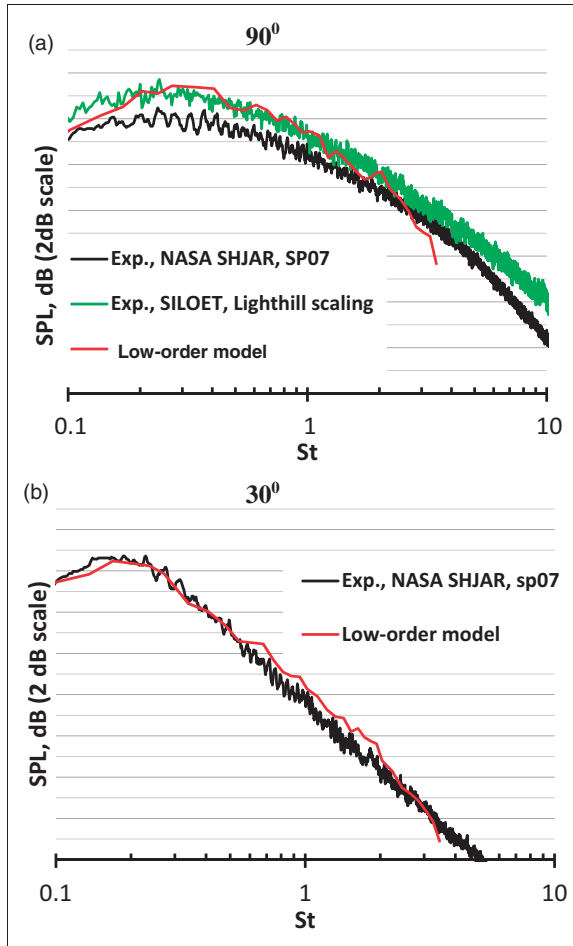
**Figure 4.** Comparison of sound spectra predictions of the new low-order model for NASA SHJAR sp07 jet, SILOET experiment data with Lighthill scaling, sJet predictions and the reference sp07 experiment data for (a) 90° and (b) 30° angle to the jet flow.
SPL: sound pressure level.

Both solutions also show a consistent 2–3 dB discrepancy with the experiment, which suggests the expected accuracy of far-field acoustic models based on the current set of LES data is 2–3 dB. This means that the observed accuracy of 1 dB for the current low-order model for predicting the NASA SHJAR sp07 spectra at small angle to the jet could be slightly fortuitous. Nevertheless, it is important to note that the 2–3 dB accuracy of the current low-order model has been achieved by using the standard scaling of the source terms and without any additional fine tuning or calibration.

Next, the acoustic modelling results for sp03 case ($M_a = 0.5$) are presented. As discussed in 'Acoustic source scaling' section, this jet case represents a strong test for the acoustic analogy model since the reference LES data are anchored at $M_a = 0.875$. Figure 7(a) and (b) shows the far-field spectra predictions of the new low-order model for the NASA SHJAR sp03 experiment for 90° and 30° observer angle to the jet flow, respectively.
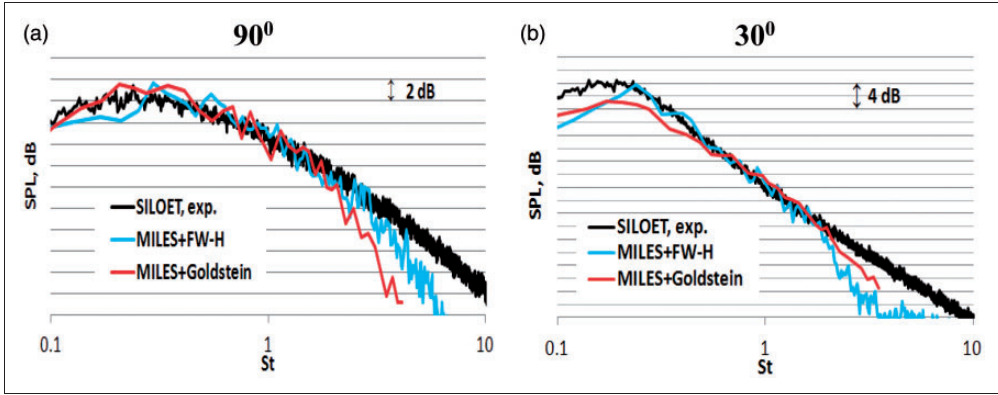
**Figure 5.** Comparison of sound spectra predictions of the Goldstein analogy implementation based on the CABARET MILES solution from Semiletov et al. (2015), the Ffowcs Williams–Hawkings solution based on the same LES data, and the reference data from the SILOET experiment for (a) 90° and (b) 30° angle to the jet flow.
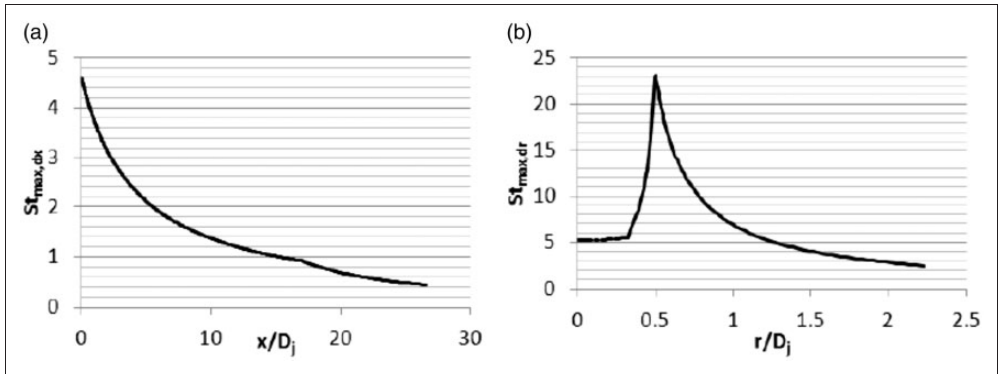SPL: sound pressure level.



**Figure 6.** Highest resolved acoustic frequencies based on 10 grid cells per acoustic wavelength for the cylindrical LES grid from Semiletov et al. (2015) in the axial (a) and radial grid direction (b).

Results of applying the Lighthill scaling to the SILOET experiment data are shown in Figure 7(a) for 90° angle for comparison. Both the acoustic analogy models, the one based on the Goldstein acoustic analogy and the one based on the Lighthill scaling, are very close and are within 2–3 dB from the experiment for this angle.

For 30°, which corresponds to the peak sound radiation angle, the predictions of the new low-order acoustic analogy model also remain within approximately 3 dB from the reference NASA experiment for peak noise frequencies. For high frequencies $St > 0.4$ and the same polar angle, the predictions of the acoustic model are within 1 dB from the experiment. Figure 7(c) shows that, for 30° angle, the predictions of the current acoustic analogy model are also very close to the predictions of the empirical sJet model.
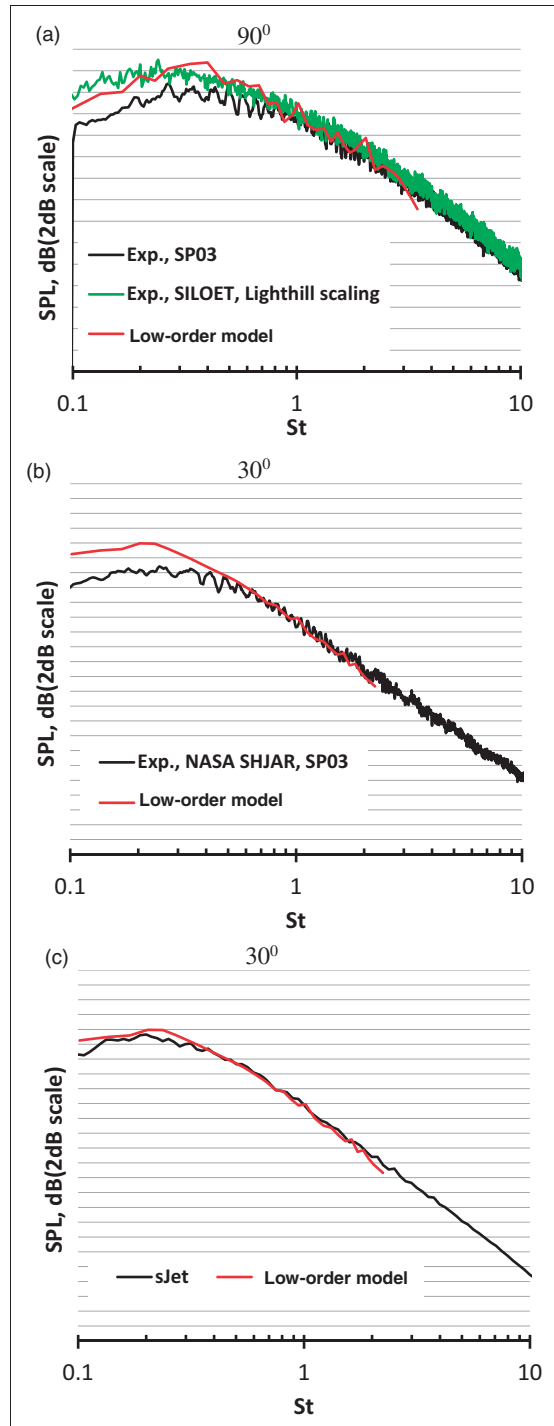
**Figure 7.** Comparison of sound pressure spectra predictions of the new low-order model for NASA SHJAR sp03 jet, SILOET experiment data with Lighthill scaling, sJet predictions and the reference sp03 experiment data for (a) 90° and (b), (c) 30° angle to the jet flow.
SPL: sound pressure level.

# Conclusion

As a first step towards a low-order modelling framework that is free from calibration parameters based on far-field noise measurements and any other assumption about the noise source structure, which is not fully confirmed either from experiment or a first-principle simulation, a new low-order noise prediction scheme for isothermal jets has been implemented. The current implementation is based on the Goldstein generalised acoustic analogy and uses the database of fluctuating Reynolds stresses of the isothermal SILOET jet from Semiletov et al.[1] for reconstructing the effective noise sources. The sources are scaled in accordance with the acoustic analogy based arguments and the corresponding sound mean-flow propagation problem is solved with the frequency domain Green's function method based on the Wind-US RANS flow solutions (Towne, 2009) for each jet condition in question. It is shown that the locally parallel flow approximation used for simplified far-field sound propagation modelling in this work, which avoids any intermediate source modelling assumptions following the approach of Semiletov et al.,[1] works reasonably well for the unheated subsonic jet cases considered.

The new low-order model has been applied to two isothermal static jet cases, sp07 and sp03, from Bridges and Wernet (2010), which correspond to acoustic Mach numbers 0.9 and 0.5, respectively. The sound spectra predictions of the new low-order scheme are broadly within 3 dB from the experiment similar to the reference solutions produced by the sJet code[30] that is empirical in nature.

In comparison with the sJet code, the new low-order jet noise prediction scheme based on the acoustic analogy is physically grounded. In comparison with the standard Lighthill scaling, the model developed is more robust as well as more physically insightful since it explicitly accounts for meanflow propagation effects. Furthermore, in comparison with previous RANS-based works based on acoustic analogies such as the ones by Khavaran et al.[20] and Leib and Goldstein,[21] the new low-order jet noise prediction scheme does not contain any calibration parameter based on the far-field data.

Further work will include developing the extensions of the new far-field calibration free low-order model, which are based on taking into account the frequency-dependent correlation lengthscales and their anisotropy. Further work will also be directed towards the use of fast-turn-around-time RANS solutions to replace the current LES database of turbulent stresses of the SILOET jet for the effective sound source reconstruction. Following the approach pursued by many researchers in the past, the future work will be based on the acoustic analogy while the difference will be in applying the source – propagation decomposition based on the LES data at the source, where the propagation effects are explicitly included and any source term calibrations based on the far-field data are avoided.

## Declaration of conflicting interests

## Funding

## References

1. Abramovich GN. The theory of turbulent jets. [English transl.] MIT Press, 1960 [AQ4].
2. Witze PO. Centerline velocity decay of compressible free jets. *AIAA J* 1974; 12: 417–418.
3. Kerherve F, Jordan P, Gervais Y, et al. Two-point laser Doppler velocimetry measurements in a Mach 1.2 cold supersonic jet for statistical aeroacoustic source model. *Expt Fluids* 2004; 37: 419 [AQ5].
4. Goloviznin VM and Samarskii AA. Finite difference approximation of convective transport equation with space splitting time derivative. *J Matem Mod* 1998; 10: 86–100.
5. Karabasov SA and Goloviznin VM. Compact accurately boundary adjusting high-REsolution technique for fluid dynamics. *J Comput Phys* 2009; 228: 7426–7451.
6. Faranosov GA, Goloviznin VM, Karabasov SA, et al. CABARET method on unstructured hexahedral grids for jet noise computation. *Comput Fluids* 2013; 88: 165–179.
7. Semiletov VA, Karabasov SA, Chintagunta A, et al. Empiricism-free noise calculation from LES solution based on Goldstein generalized acoustic analogy: volume noise sources and meanflow effects. In: *21st AIAA/CEAS aeroacoustics conference*, AIAA Aviation, AIAA 2015–2536.
8. Lighthill MJ. On sound generated aerodynamically: I. *General theory*. Proc Royal Soc London A 1952; 222: 564–587.
9. Lilley GM. On the noise from air jets. *Aeronaut Res Council Rep Mem* 1958; 20: 376.
10. Ffowcs Williams JE. The noise from turbulence convected at high speed. *Phil Trans Roy Soc London* 1963; 255: 469–503.
11. Ribner HS. The generation of sound by turbulent jets. *Adv Appl Mech* 1964; 8: 108–182.
12. Tester BJ and Morfey CL. Development in jet noise modelling—Theoretical predictions and comparisons with measured data. *J Sound Vib* 1976; 46: 79–103.
13. Goldstein ME. A generalized acoustic analogy. *J Fluid Mech* 2003; 488: 315–333.
14. Goldstein ME and Leib SJ. The aero-acoustics of slowly diverging supersonic jets. *J Fluid Mech* 2008; 600: 291–337.
15. Harper-Bourne M. Jet noise turbulence measurements. In: *AIAA paper 2003–3214*, 2003.
16. Morris PJ and Zaman KBMQ. Velocity measurements in jets with application to noise source modeling. *J Sound Vib* 2010; 329: 394–414.
17. Karabasov SA, Afsar MZ, Hynes TP, et al. Jet noise: Acoustic analogy informed by large Eddy simulation. *AIAA J* 2010; 48: 1312–1325.
18. Leib SJ, Ingraham D and Bridges JE. Evaluating source terms of the generalized acoustic analogy using the Jet Engine Noise REduction (JENRE) Code. In: *55th AIAA aerospace sciences meeting*, AIAA SciTech Forum, AIAA 2017-0459.
19. Khavaran A, Bridges J and Georgiadis N. *Prediction of turbulence-generated noise in unheated jets*. 2005 [AQ6].
20. Khavaran A, Kenzakowski DC and Mielke-Fagan AF. Hot jets and sources of jet noise. *Int J Aeroacoust* 2010; 9: 491–532.

21. Leib SJ and Goldstein ME. Hybrid source model for predicting high-speed jet noise. *AIAA J* 2011; 49: 1324–1335.
22. Karabasov SA, Bogey C and Hynes TP. An investigation of the mechanisms of sound generation in initially laminar, subsonic jets using the Goldstein acoustic analogy. *J Fluid Mech* 2013; 714: 24–57.
23. Bassetti A and Nichols JW. Analysis of LES for source modeling in jet noise. In: *20th AIAA/CEAS aeroacoustics conference*, AIAA Aviation, AIAA 2014-2905.
24. Karabasov SA and Sandberg RD. Influence of free stream effects on jet noise generation and propagation within the Goldstein acoustic analogy approach for fully turbulent jet inflow boundary conditions. *Int J Aeroacoust* 2015; 14: 413–429.
25. Kreitzman JR and Nichols JW. Acoustic source analysis of a supersonic rectangular chevron jet. In: *21st AIAA/CEAS aeroacoustics conference*, Dallas, TX, 2015.
26. Bridges J and Wernet MP. Establishing consensus turbulence statistics for hot subsonic jets. In: *AIAA paper 2010–3751*, 2010.
27. Towne CE. *Wind-US users guide*. Version 2.0. October 2009.
28. Tam CKW and Auriault L. Mean flow refraction effects on sound from localized sources in a jet. *J Fluid Mech* 1998; 370: 149–174.
29. Semiletov VA and Karabasov SA. On the properties of turbulent fluctuating stress sources for high-speed jet noise. In: *22nd AIAA/CEAS aeroacoustics conference*, 2016.
30. Khavaran A and Bridges J. *An empirical temperature variance source model in heated jets*. 2012.
31. Viswanathan K. Mechanisms of jet noise generation: classical theories and recent developments. *Int J Aeroacoust* 2009; 8: 355–407.